

Modeling and Nonlinear Control of an Electrohydraulic Closed-Center Power-Steering System

Wolfgang Kemmetmüller, Andreas Kugi
Chair of System Theory and Automatic Control
Saarland University
Saarbruecken, Germany
Email: andreas.kugi@lrs.uni-saarland.de

Steffen Müller
Vehicle Dynamics Control Systems
BMW Group
Munich, Germany

Abstract—This paper deals with the mathematical modeling and the nonlinear control of an electrohydraulic closed-center power-steering system. The system under consideration is characterized by its high energetic efficiency at a full electric power-steering functionality. Based on a nonlinear mathematical model of the system, a flatness-based controller for the servo actuator is designed. Afterwards, an interpretation of the overall steering control system as a mechanical impedance matching problem yields a controller with good performance and robust behavior. Finally, measurement results on a test stand and in a test car show the usefulness of the proposed control approach.

I. INTRODUCTION

Present hydraulic power-steering systems do not meet the requirements of future steering systems anymore. Increasing demands on driving dynamics, ride comfort and ride stability as well as tighter restrictions on the fuel consumption demand new approaches, see, e.g., [15]. As a result, new steering systems like electrohydraulic power-steering (EHPS) and electric power-steering (EPS) systems have recently been introduced in the market, see, e.g., [8], [17]. For both systems the power is supplied by the electric power supply of the vehicle. For driving situations with high steering assistance this involves large electric currents. As the steering assistance grows with the size of the car, up to now these systems are limited to small and middle class cars. Many works dealing with the control of EPS and EHPS systems have been published in the last years, most of them based on linear (optimal, adaptive) control approaches, see, e.g., [6], [11], [16] and [17] for EPS and [1] and [8] for EHPS systems.

In this paper, we will analyze a closed-center power-steering system consisting of an energetically optimized belt driven hydraulic power supply and two closed-center steering valves. This configuration is capable of fulfilling the power demands on high steering assistance even for luxury class cars, while ensuring less fuel consumption compared to conventional hydraulic power steering systems. Furthermore, it is possible to actively influence the steering dynamics. The main focus of the paper is laid on a controller design for the steering system. Thereby, the controller has to cope with the inherent nonlinear behavior arising in hydraulic systems, e.g., due to the valve opening characteristics, see, e.g., [14]. Since we assume that the hydraulic power supply is able to provide a sufficiently large system pressure, we will keep

the description of the hydraulic power supply system to a necessary minimum.

The paper is organized as follows: In Section II we will present a schematic diagram of the overall steering system. Afterwards, we will derive a detailed mathematical model of the system. Section III is devoted to the controller design. First, we will determine a flatness-based controller for the servo force and then the controller for the steering torque will be designed. Furthermore, essential issues like the steering feeling and the stability will be addressed in this section. Measurement results performed on a hardware in the loop (HIL) test stand will be shown in Section IV. In the last section, Section V, we will summarize the results and give a short outlook on future research activities.

II. MATHEMATICAL MODELING

A. System Overview

Fig. 1 depicts a schematic diagram of the electrohydraulic closed-center steering system. It can be formally subdivided into four subsystems: (i) the mechanical steering system consisting of the steering wheel, the steering column, the torsion bar and the steering rack; (ii) the hydraulic steering assistant system comprising the assistant cylinder and the steering valves (volume flows q_A and q_B); (iii) the hydraulic power supply built up by a constant displacement pump, an electronically controlled inlet orifice, a proportional bypass valve and a hydraulic accumulator and (iv) the electronic control unit (ECU) with the related sensors for the pressures in the two chambers, p_A and p_B , as well as the supply pressure p_S , the steering wheel angle φ_{SW} and the steering torque τ_{SC} . The principle mode of operation can be summarized as follows. If the driver turns the steering wheel, the torsion bar is twisted and a steering torque is generated, which in turn moves the steering rack. Depending on the change in the steering rack position s (velocity $w = \dot{s}$) the direction of travel of the vehicle changes which causes a change in the rack force f_{rack} . With no servo force applied by the assistant cylinder, the rack force would equal the steering force f_{SC} which is equivalent to the steering torque $\tau_{SC} = f_{SC}/i$, with the gear transmission ratio i . In order to assist the driver and to provide a good steering feeling, a certain amount of the rack force is compensated by the servo

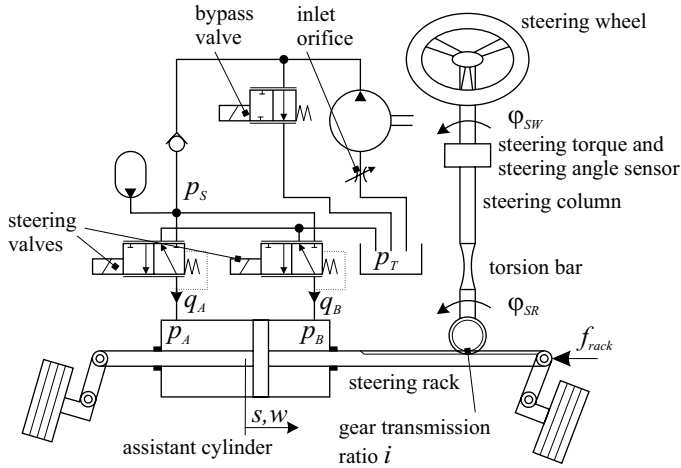


Fig. 1. Schematic diagram of the overall steering system.

force $f_{servo} = (p_A - p_B) A_{AC}$ generated by the assistant cylinder, with A_{AC} as the effective piston area.

B. Mechanical Steering System

The steering wheel is connected to the steering rack via the steering torque sensor, the steering column, the torsion bar and a gearbox. Both, the torsion bar and the torque sensor, can be modeled in the form of linear springs with stiffness c_{TB} and c_{TS} , respectively. Due to the fact that the moment of inertia of the steering column is small compared to that of the steering wheel θ_{SW} , the steering column can be modeled in the form

$$\theta_{SW} \ddot{\varphi}_{SW} = \tau_{driver} - \tau_{SC}, \quad (1)$$

where τ_{driver} denotes the torque on the steering wheel enforced by the driver and τ_{SC} is given by

$$\tau_{SC} = c_{SC} (\varphi_{SW} - \varphi_{SR}) + \tau_{d,SC}. \quad (2)$$

Here $c_{SC} = (c_{TB} c_{TS}) / (c_{TB} + c_{TS})$ is the effective stiffness of the steering column and $\tau_{d,SC} = d_{v,SW} \dot{\varphi}_{SW} + d_{c,SW} \text{sign}(\dot{\varphi}_{SW})$ denotes the friction, where $d_{v,SW}$ is the viscous and $d_{c,SW}$ the Coulomb friction coefficient.

The systematic determination of the driver's torque τ_{driver} is a controversial problem. On the one hand the driver clearly applies a torque to the steering wheel via his/her hands and arms. On the other hand, normally the driver wants the vehicle to follow a specific path (i.e. the road) which results in a desired steering wheel angle φ_{SW}^* . This also implies that the driver tries to control the driver's torque in such a way that the desired steering wheel angle is achieved. A mathematical model of the driver's behavior is evidently very complex and beyond the scope of this paper, see, e.g., [13] and the references cited therein for more details on this topic. Nonetheless, for simulation purposes we make the assumption that the driver is able to control the steering angle fast enough. Thus, we can take the (desired) steering wheel angle as the driver's input to the steering system. Then the driver's torque can simply be calculated by means of (1).

In the following, we will design a steering assistance strategy based on a controller for the steering torque τ_{SC} instead of the driver's torque τ_{driver} , since (i) these two quantities are equivalent in the stationary case and (ii) the resulting torque due to an acceleration of the wheel $\ddot{\varphi}_{SW} \theta_{SW}$ is considered negligible for characteristic steering maneuvers.

The mathematical model of the steering rack reads as

$$\begin{aligned} \dot{s} &= w \\ m_{SR} \dot{w} &= f_{servo} + \tau_{SC} i - f_{fric} - f_{rack}, \end{aligned} \quad (3)$$

with the mass m_{SR} of the steering rack and all masses rigidly connected to it, the servo force f_{servo} , the steering force $f_{SC} = \tau_{SC} i$ and the friction force f_{fric} . The rack force f_{rack} denotes the sum of all reaction forces of the vehicle. Many works dealing with a detailed calculation of the dynamic reaction forces of the car have been published, see, e.g., [13]. In this work the simulation model of the rack force is based on a simple single-track model which gives good results for stable driving conditions. The major part of the friction force f_{fric} results from the sealings of the assistant cylinder. As the sealings are forced against the walls of the cylinder by the pressures in the chambers, the friction increases with the sum pressure, i.e. $f_{fric} = d_{c,SR} (p_A + p_B) \text{sign}(w) + d_{v,SR} w$. Here $d_{c,SR} (p_A + p_B)$ denotes the pressure dependent Coulomb friction coefficient and $d_{v,SR}$ is a viscous friction coefficient.

C. Hydraulic Assistant System

The steering assistant force f_{servo} is generated by means of a double rod cylinder. The pressures p_A and p_B in the chambers A and B of the cylinder, cf. Fig. 1, are given by

$$\dot{p}_A = \frac{\beta}{V_{AC} + A_{AC} s} (-A_{AC} w + q_A) \quad (4a)$$

$$\dot{p}_B = \frac{\beta}{V_{AC} - A_{AC} s} (A_{AC} w + q_B), \quad (4b)$$

where β denotes the bulk modulus of the oil and V_{AC} the volume of the cylinder chambers for $s = 0$. The volume flows q_A and q_B are supplied by two steering valves, which in our case are built up in the form of pressure control valves. Fig. 2 shows a schematic diagram of the pressure control valve designed by HYDAC ELECTRONIC GMBH [9]. In the following we will only describe the valve A, since the equations for valve B are identical. The valve

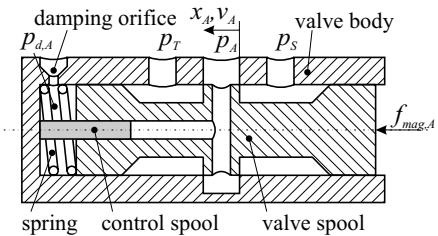


Fig. 2. Schematic diagram of the pressure control valve [9].

consists of a valve spool which is controlled by the magnetic force $f_{mag,A}$ generated by a solenoid. A current control

loop imposes the current i_A on the solenoid and assures a very fast dynamics of the electric subsystem of the valve. Therefore, the magnetic force can be modeled in form of a static nonlinear relationship with i_A as the control input, i.e., $f_{mag,A} = f_{mag,A}(i_A)$. The restoring of the valve spool is ensured by a spring with the force $f_{c,A} = c_v x_A + f_0$, where c_v denotes the spring stiffness, x_A the position of the valve spool and f_0 the bias force. Furthermore, the control spool with the effective area A_{CS} generates a restoring force $p_A A_{CS}$ being proportional to the chamber pressure p_A . The friction force $f_{f,A}$ comprises the mechanical friction and the hydraulic damping

$$f_{f,A} = d_{v,v} v_A + d_{c,v} \text{sign}(v_A) + f_{d,A}, \quad (5)$$

with the viscous friction coefficient $d_{v,v}$, the Coulomb friction coefficient $d_{c,v}$ and the velocity of the valve spool v_A . Stick-slip effects do not play a role in our case since the electric current loop consists of a pulse-width-modulation controlled system. Thereby, the carrier frequency is chosen in such a way that the induced current ripple prevents the valve spool from sticking. The hydraulic damping force $f_{d,A}$ is generated by a damping orifice. The motion of the valve spool induces a volume flow proportional to the valve spool velocity v_A , which in turn generates a damping force in the form of $f_{d,A}(v_A)$, see, e.g., [3] for more details.

While in multi-stage servo valves jet forces can be neglected, they have a great influence in conventional pressure control valves. Jet forces always occur if oil flows over the control edges either from the pressure supply to the chamber (volume flow q_{SA}) or from the chamber to the tank (volume flow q_{AT}). The volume flows are given by

$$\begin{aligned} q_{SA} &= \alpha \sqrt{\frac{2}{\rho}} A_{SA}(x_A) \sqrt{p_S - p_A} \\ q_{AT} &= \alpha \sqrt{\frac{2}{\rho}} A_{AT}(x_A) \sqrt{p_A - p_T}, \end{aligned} \quad (6)$$

where α is the constant discharge coefficient and $A_{SA}(x_A)$ and $A_{AT}(x_A)$ denote the opening characteristics of the valve from supply to chamber and from chamber to tank, respectively. Since the opening characteristics, $A_{SA}(x_A)$ and $A_{AT}(x_A)$, do have an essential influence on the dynamic behavior, an accurate modeling is absolutely necessary. It turns out that we have to use piecewise defined polynomials at least of order 3 to get a satisfactory approximation. In our application we use critical center valves, i.e. $A_{SA}(x_c) = A_{AT}(x_c) = 0$, where x_c denotes the middle position of the valve spool. Thus, the volume flow into the chamber directly results in $q_A = q_{SA} - q_{AT}$. Using the relations of e.g., [2], [3], we can calculate the jet forces by

$$f_{jet,A} = \sqrt{2\rho} (q_{SA} \sqrt{p_S - p_A} - q_{AT} \sqrt{p_A - p_T}) \cos(\theta), \quad (7)$$

where the density of the oil ρ and the jet angle θ are assumed to be constant. The overall model of the pressure control valve is completed by the equations of motion of the valve spool of mass m_v :

$$\begin{aligned} \dot{x}_A &= v_A \\ m_v \dot{v}_A &= f_{mag,A} - p_A A_{CS} - f_{jet,A} - f_{c,A} - f_{f,A} \end{aligned} \quad (8)$$

D. Hydraulic Power Supply

The key point in the design of a high efficient power supply is the inclusion of a hydraulic accumulator for the storage of hydraulic energy. This hydraulic accumulator allows us to temporarily shut down the pump by means of the inlet orifice and the bypass valve when only little volume flow is necessary.

III. CONTROLLER DESIGN

The controller design proceeds in two steps. First, we design a flatness-based controller for the pressures in the chambers of the assistant cylinder. Together with a trajectory generator, taking the desired servo force f_{servo}^* as the control input, they form the inner control loop of the system. Then, for the outer control loop we develop an impedance controller to provide a good steering feeling.

A. Pressure Controller

For the controller design of the chamber pressure p_A let us reconsider the mathematical model (4a), (8) by neglecting the Coulomb friction. If we assume zero velocity of the steering cylinder $w = 0$ and a constant magnetic force $f_{mag,A}^*$ (i.e. a constant input current i_A^*), then the set of equilibrium points is given by $\varepsilon = \{\bar{x}_A = x_c, \bar{v}_A = 0, \bar{p}_A\}$, with

$$A_{CS} \bar{p}_A = f_{mag,A}^* - c_v x_c - f_0. \quad (9)$$

It can be shown that the equilibrium is asymptotically stable in the sense of Lyapunov, provided that the parameters, in particular the effective area of the control spool A_{CS} , are lying within certain limits. Note that the control spool is nothing else than a mechanically implemented proportional controller where the effective area of the control spool A_{CS} corresponds to the proportional gain.

For the design of a tracking controller we take advantage of the differential flatness of (4a), (8), see, e.g., [4] for the background on the notion of flatness. Roughly speaking, this property ensures that, given a flat output ξ_1 (in our case p_A), the state $\mathbf{x} = [p_A, x_A, v_A]$ and the input $f_{mag,A}$ can be determined by the flat output and its time derivatives. Furthermore, this design allows us to systematically include the (known) exogenous variables $s(t)$, $\dot{s}(t) = w(t)$ in the controller design. Let $\xi_1^* = p_A^*(t) \in C^3$ denote the three times continuously differentiable desired trajectory for the chamber pressure p_A . Then the first derivative with respect to time is given by

$$\dot{\xi}_1^* = \xi_2^* = \frac{\beta}{V_{AC} + A_{ACS}} (-A_{AC} w + q_A), \quad (10)$$

with $q_A = q_A(\xi_1^*, x_A^*)$ given by (6). For the sake of convenience let $x_A^* = \chi_1^*(\xi_1^*, \xi_2^*, s, w)$ denote the solution of (10). Onward differentiation gives

$$\dot{\xi}_2^* = \xi_3^* = \frac{\partial \xi_2^*}{\partial \xi_1^*} \xi_2^* + \frac{\partial \xi_2^*}{\partial x_A^*} \dot{x}_A^* + \frac{\partial \xi_2^*}{\partial s} w + \frac{\partial \xi_2^*}{\partial w} \dot{w}, \quad (11)$$

where $\dot{x}_A^* = v_A^*$ is the velocity of the valve spool. For a condensed notation we will henceforth use the abbreviations $\Xi = \{\xi_1, \xi_2, \xi_3\}$ and $\vartheta = \{s, w, \dot{w}\}$. Then

$v_A^* = \chi_2^*(\Xi^*, s, w, \dot{w})$ denotes the solution of (11). The third derivative

$$\begin{aligned} \dot{\xi}_3^* &= \sum_{i=1}^2 \frac{\partial \xi_3^*}{\partial \xi_i^*} \xi_{i+1}^* + \frac{\partial \xi_3^*}{\partial x_A^*} v_A^* + \frac{\partial \xi_3^*}{\partial v_A^*} \dot{v}_A^* \\ &+ \sum_{i=1}^3 \frac{\partial \xi_3^*}{\partial \vartheta_i} \vartheta_{i+1} = \psi(\Xi^*, f_{mag,A}^*, \vartheta) \end{aligned} \quad (12)$$

finally includes the input, since

$$\begin{aligned} m_v \dot{v}_A^* &= f_{mag,A}^* - \xi_1^* A_{CS} - c_v x_A^* \\ &- f_{jet,A}(\xi_1^*, x_A^*) - f_{f,A}(v_A^*) - f_0. \end{aligned} \quad (13)$$

Combining (12) and (13) and solving for $f_{mag,A}^*$, we get the flatness-based feedforward control in the form of

$$f_{mag,A}^* = \chi_3^*(\Xi^*, \dot{\xi}_3^*, \vartheta). \quad (14)$$

If the desired trajectory $\xi_1^*(t)$ of the flat output is consistent with the initial condition \mathbf{x}_0 , then the output $p_A(t)$ exactly tracks the desired output, provided that the mathematical model is exact. Moreover, by a simple change of coordinates the system (4a) and (8) with the feedforward control for the valve A due to (14) can be written in Brunovsky form, see, e.g., [10], [7]

$$\dot{\xi}_1 = \xi_2, \quad \dot{\xi}_2 = \xi_3, \quad \dot{\xi}_3 = \dot{\xi}_3^*. \quad (15)$$

In order to cope with model uncertainties and inconsistent initial conditions we have to incorporate a feedback control to stabilize the tracking error $\mathbf{e} = \Xi - \Xi^*$. For this purpose we take advantage of the fact that the following property holds [7]: If the desired trajectory of the flat output is not consistent with the initial condition \mathbf{x}_0 , but it is sufficiently close to the initial condition, then, when applying the feedback control, there exists a unique solution at least for a given finite time interval in the vicinity of the desired trajectory, which represents the solution of the aforementioned Brunovsky form. This observation in combination with an extended control law in the form of

$$f_{mag,A} = \chi_3^*(\Xi^*, \dot{\xi}_3^* - \Lambda(\mathbf{e}), \vartheta) \quad (16)$$

yields a closed-loop error system

$$\begin{aligned} \dot{e}_i &= e_{i+1}, \quad i = 1, 2 \\ \dot{e}_3 &= \psi(\Xi, \chi_3^*(\Xi^*, \dot{\xi}_3^* - \Lambda(\mathbf{e}), \vartheta), \vartheta) - \dot{\xi}_3^*. \end{aligned} \quad (17)$$

Now a PID-like feedback law given by

$$\Lambda(\mathbf{e}) = \lambda_0 \int_0^t e_1(\tau) d\tau + \sum_{i=1}^3 \lambda_i e_i, \quad \lambda_i > 0, \quad i = 0, \dots, 3 \quad (18)$$

can be used to stabilize the error dynamics (17). The proof of the stability relies on the linearized, time varying closed-loop error system, see, e.g., [7] and [12].

Remark 1: A state feedback law (18) requires the knowledge of the full state \mathbf{x} . In our application only p_A can be measured. In [5] an estimation of the time derivatives of the flat output based on a polynomial representation of the flat output is proposed. With this approach the time derivatives can be calculated in a robust way by means of time varying

linear filters. In our case it turns out that a partial state feedback law in the form of

$$\Lambda(\mathbf{e}) = \lambda_0 \int_0^t e_1(\tau) d\tau + \lambda_1 e_1, \quad \lambda_i > 0, \quad i = 0, 1 \quad (19)$$

is sufficient for the stabilization of the system. For a proof of the stability the linearization of the corresponding closed-loop error system has to be performed. Due to the aforementioned piecewise approximation of the nonlinear opening characteristics of the valve it is not possible to determine this linearization analytically. This is why we are not able to give a rigorous proof of the stability for the proposed pressure controller. Nevertheless, excessive simulation studies and measurements in a test car show a very robust behavior w.r.t. model uncertainties and inconsistent initial conditions.

Remark 2: The proposed feedforward controller (14) uses the exogenous variable $s(t)$ and its derivatives up to the order 3. Although the position $s(t)$ of the assistant cylinder cannot be measured it can be approximately derived from the measured steering wheel angle φ_{SW} and the steering torque τ_{SC} by the relation $\tau_{SC} = c_{SC}(\varphi_{SW} - is)$. Again, the time derivatives can be determined e.g. by the approach of [5] or by approximate differentiation. However, in our application \dot{w} and \ddot{w} are considerably small and will therefore be neglected in (14) or (16), respectively.

The controller for the second chamber B is completely equivalent to the one of chamber A if one replaces s by $-s$ and consequently w by $-w$. In order to complete the inner control loop the desired servo force $f_{servo}^* = A_{AC}(p_A^* - p_B^*)$, determined by the outer control loop, has to be subdivided into the two trajectories for the chamber pressures p_A^* and p_B^* , respectively. It is immediately evident that by the choice of f_{servo}^* the chamber pressures are not fixed. Thus, this extra degree-of-freedom is utilized to keep the sum pressure $p_A^* + p_B^*$ as small as possible in order to minimize the friction in the assistant cylinder.

B. Steering Torque Controller

When dealing with power steering systems, the main challenge in the design of a steering torque controller is to provide a good steering feeling. Unfortunately, this term is very subjective since every car manufacturer has its own definition of good steering feeling. Nonetheless, the essential requirements of all power steering systems are equal. First of all, the power steering system has to provide a sufficient assistance to the driver. This is especially the case for low velocities, where the rack forces are very high. Secondly, in modern power steering systems, the level of assistance is varied with the vehicular velocity. This means that for low velocities much assistance should be provided to allow for low steering effort (e.g. during parking maneuvers), while the steering torque should be higher to ensure save driving for higher velocities. Finally, the power steering system must not cause unusual steering behaviors (like, e.g., opposing the driver's request) and the stability of the system has to be guaranteed in all driving conditions.

In our work we will tackle the steering torque controller design by means of a mechanical impedance matching task.

This approach has the advantage that the solution of providing an appropriate steering feeling can be found almost independently from the stability problem. For this purpose let us first formulate the transformed equations for the steering rack in the new coordinates $\Delta\varphi = \varphi_{SW} - \varphi_{SR}$, $\varphi_{SR} = i s$

$$\begin{aligned}\Delta\dot{\varphi} &= \Delta\omega \\ \Delta\dot{\omega} &= \ddot{\varphi}_{SW} - \frac{i^2}{m_{SR}} (\tau_{servo} + \tau_{SC} - \tau_{load}),\end{aligned}\quad (20)$$

with the servo torque $\tau_{servo} = f_{servo}/i$ and the load torque $\tau_{load} = (f_{fric} + f_{rack})/i$ including both the rack force f_{rack} and the friction force f_{fric} . The basic idea is that (20) is controlled by the control input τ_{servo} in such a way that in response to a load torque τ_{load} the controlled closed-loop system acts in the same way as a desired mechanical impedance system. In a first view it seems somehow odd that we address the steering feeling issue by an impedance system taking the load force τ_{load} and not the steering torque τ_{SC} as input. But we will show later on how this is linked to the control of the steering torque. The desired impedance system can then be written as

$$\begin{aligned}\Delta\dot{\varphi} &= \Delta\omega \\ \Delta\dot{\omega} &= -\frac{i^2}{m_{SR}} (\Lambda_c(\Delta\varphi) + \Lambda_d(\Delta\omega) - \tau_{load}),\end{aligned}\quad (21)$$

where $\Lambda_c(\Delta\varphi)$ can be viewed as the desired (nonlinear) spring characteristics and $\Lambda_d(\Delta\omega)$ as the desired (nonlinear) damping characteristics. Comparing (20) and (21) the matching condition reads as

$$\tau_{servo} = \frac{m_{SR}}{i^2} \ddot{\varphi}_{SW} - \tau_{SC} + \Lambda_c(\Delta\varphi) + \Lambda_d(\Delta\omega). \quad (22)$$

It can be seen that in (21) the steering torque τ_{SC} no longer appears explicitly. The driver's control reenters the system via the difference angle $\Delta\varphi$ which can be written as $\Delta\varphi = \tau_{SC}/c_{SC}$ provided that the damping torque $\tau_{d,SC}$ is assumed to be zero, cf. (2).

Let us now analyze the simplest case of only applying a linear spring of stiffness κ , i.e. $\Lambda_c(\Delta\varphi) = \kappa\Delta\varphi$ and $\Lambda_d(\Delta\omega) = 0$. Under the assumption that the acceleration of the steering wheel can be neglected, i.e. $\ddot{\varphi}_{SW} = 0$, the servo torque is given by $\tau_{servo} = -\tau_{SC} + \kappa\tau_{SC}/c_{SC}$. Inserting this expression in (20), we get in the quasi-stationary case $\tau_{SC} = (c_{SC}/\kappa)\tau_{load}$. From this we can see that for high steering assistance, i.e. $\tau_{SC} \ll \tau_{load}$, large values of κ are mandatory. If we now keep in mind a finite dynamics of the inner control loop, it can be shown that this control loop as a matter of principle tends to be unstable for high steering assistance, see also [6] for similar observations. To overcome this stability problem let us for the time being assume that we can measure the load torque τ_{load} . The introduction of a disturbance feedforward of the form $\tau_{servo} = \tilde{\tau}_{servo} + \Gamma(\tau_{load})$ with $|\Gamma(\tau_{load})| < |\tau_{load}|$ in (20) can be used to systematically compensate a part of the load force. It can be easily seen that with the transformed load input $\tilde{\tau}_{load} = \tau_{load} - \Gamma(\tau_{load})$ we obtain the similar impedance matching problem as before. For the case of a linear spring of stiffness $\tilde{\kappa}$ we then get $\tilde{\tau}_{servo} = -\tau_{SC} + \tilde{\kappa}\tau_{SC}/c_{SC}$. Again this yields the

following relation $\tau_{SC} = (c_{SC}/\tilde{\kappa})(\tau_{load} - \Gamma(\tau_{load}))$ in the quasi-stationary case. For the sake of simplicity let us take $\Gamma(\tau_{load}) = \gamma\tau_{load}$ where $0 \leq \gamma \leq 1$. Since we want the transformed system to behave equally to the original system the relation $(c_{SC}/\kappa)\tau_{load} = (c_{SC}/\tilde{\kappa})(1 - \gamma)\tau_{load}$ has to be fulfilled. Obviously, a suitable choice of γ brings about that $\tilde{\kappa} = (1 - \gamma)\kappa \ll \kappa$ and thus the stability problems occurring for high steering assistance as mentioned above can be circumvented. However, this is due to the fact that the main part of the load torque τ_{load} is compensated by a disturbance feedforward $\gamma\tau_{load}$ and the impedance matching controller only has to cope with the small difference $\tilde{\tau}_{load} = (1 - \gamma)\tau_{load}$. Of course this methodology is not limited to the simple case of a linear spring characteristics as discussed so far. Indeed we can apply an almost arbitrary (nonlinear) assistant characteristics which can also be a function of other variables, like e.g. the vehicular velocity. The price we have to pay is that we additionally need the information of the load torque. Clearly, in general neither the load force nor the load torque is measurable. For this reason we use an observer which determines an estimation $\hat{\tau}_{load}$ of τ_{load} . At the moment a rigorous stability proof for the closed-loop system consisting of the inner pressure control loop and the outer impedance controller together with the load estimator and the disturbance feedforward is not available and has to be further examined. Nevertheless, simulation and measurement results prove the feasibility and also the robustness of the proposed concept.

Remark 3: The design of the desired impedance system in the difference angle $\Delta\varphi = \varphi_{SW} - \varphi_{SR}$ is crucial. If we would try to enforce an impedance system in φ_{SR} it can be immediately seen that the driver's demand would be completely cancelled out. If on the other hand we would try to design an impedance system in the steering wheel angle φ_{SW} , all load forces and therefore all informations from the road are cancelled out which is undesirable as well.

IV. EXPERIMENTAL RESULTS

For testing the proposed control strategy a hardware in the loop (HIL) test stand and a test car have been set up at BMW AG MUNICH. The control concept is implemented in a DSPACE realtime hardware at a sample time of 1 ms. On the HIL test stand the dynamics of the car is simulated by a force-controlled hydraulic piston actuator which introduces rack forces determined by a single-track model. While the HIL test stand makes it easily possible to optimize the controller parameters under controlled laboratory conditions with a large number of additional measurements, the optimization of the driver's feeling issues is done in the test car.

Due to space limitation we can only show a typical measurement result (Fig. 3) of the HIL test stand. In this measurement the driver tries to impose a sinusoidal steering wheel angle with increasing frequency and angle. This test scenario is used to evaluate the behavior of the power steering system in the case of fast steering wheel velocities. In this scenario the expectations of an ideal power steering system would be an almost constant steering torque. The

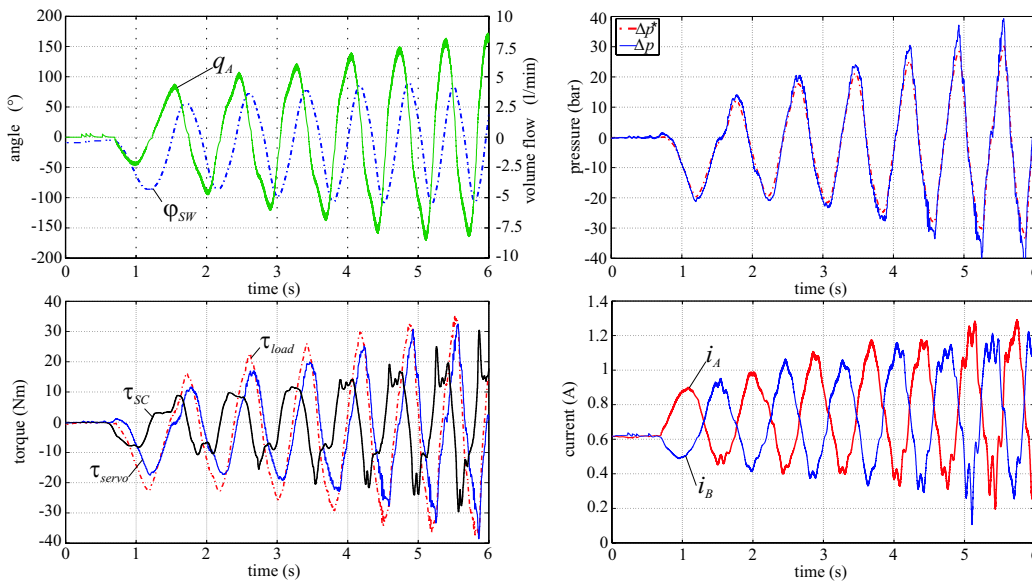


Fig. 3. Measurement results for different driving situations performed on a HIL test stand of BMW AG MUNICH.

measurements show that the steering torque τ_{SC} slowly increases with increasing frequency and steering angle. Furthermore, the difference pressure Δp shows a good tracking behavior. The overshoot occurring for high frequencies is mainly due to the influence of the jet forces inside the steering valves. Summarizing, we can say that the proposed control strategy shows a good behavior in most of the driving situations. Nonetheless, there are still critical maneuvers where the response of the system is not satisfactory, as it is e.g. the case for the higher frequencies in the sinusoidal steering scenario. This issue is currently being addressed in our research activities.

V. CONCLUSIONS AND OUTLOOK

In this contribution we presented a systematic mathematical modeling and a nonlinear controller design for an electrohydraulic closed-center power-steering system. The nonlinear controller design is based on a cascaded structure, with a flatness-based controller for the chamber pressures in the inner loop and a mechanical impedance controller for the steering torque in the outer loop. Measurement results on a HIL test stand and in a test car at BMW AG MUNICH prove the usefulness and the robustness of the proposed control approach. Future research activities include an optimization of the overall system by taking advantage of enhanced steering valves. Furthermore, an application of the proposed control concept to other EHPS systems is under investigation.

VI. ACKNOWLEDGMENT

The authors would like to thank HYDAC ELECTRONIC GMBH, in particular F. Kattler, F. Herold and T. Daniel, for the successful partnership. Further we would like to thank I. Nagy and T. Hartmann at BMW AG MUNICH for the fruitful cooperation.

REFERENCES

- [1] T. Acarman et al., A Robust Controller Design for Drive by Wire Hydraulic Power Steering System, In: *Proc. of the 2002 American Control Conference*, Anchorage, 2002.
- [2] J.F. Blackburn, G. Reethof and J.L. Shearer, *Fluid Power Control*, John Wiley & Sons, New York, 1960.
- [3] D. McCloy and H.R. Martin, *Control of Fluid Power: Analysis and Design*, John Wiley & Sons, New York, 1980.
- [4] M.J. Fliess et al., Flatness and Defect of Non-linear Systems: Introductory Theory and Examples, *Int. J. Control*, Vol. 61, No. 6, pp. 1327-1361, 1995.
- [5] M.J. Fliess and H. Sira-Ramírez, Control via State Estimations of some Nonlinear Systems, In: *Preprints of the 6th IFAC Symposium on Nonlinear Control Systems*, pp. 43-50, Stuttgart, 2004.
- [6] O. Graßmann et al., Variable Lenkunterstützung für eine elektromechanische Servolenkung, In: *Proc. of Hydraulik und Pneumatik in der Fahrzeugtechnik*, Essen, 1995.
- [7] V. Hagenmeyer, *Robust Nonlinear Tracking Control based on Differential Flatness*, VDI-Verlag, Düsseldorf, 2003.
- [8] P. Hingwe, M. Tai and M. Tomizuka, Modeling and Robust Control of Power Steering System of Heavy Vehicles for AHS, In: *Proc. of the 1999 IEEE International Conference on Control Applications*, Hawaii, 1999.
- [9] HYDAC Electronic GmbH, *Technical Documentation for Closed Center Pressure Control Valve*, internal communication, 2004.
- [10] A. Isidori, *Nonlinear Control Systems*, Springer, New York, 1995.
- [11] K. Ji-Hoon and S. Jae-Bok, Control Logic for an Electric Power Steering System using Assist Motor, *Mechatronics*, Vol. 12, pp. 447-459, 2002.
- [12] H.K. Khalil, *Nonlinear Systems, Third Edition*, Prentice Hall, Upper Saddle River, 2002.
- [13] U. Kiencke and L. Nielsen, *Automotive Control Systems*, Springer, Berlin, 2000.
- [14] A. Kugi and W. Kemmetmüller, Impedance Control of Hydraulic Piston Actuators, In: *Preprints of the 6th IFAC Symposium on Nonlinear Control Systems*, pp. 1241-1246, Stuttgart, 2004.
- [15] S. Müller, A. Kugi and W. Kemmetmüller, Analysis of a Closed-Center Hydraulic Power Steering for Full Steer-by-Wire Functionality and Low Fuel Consumption, In: *Proc.-CD of the 9th Scandinavian International Conference on Fluid Power*, Linköping, Sweden, 2005.
- [16] N. Sugitani et al., Electric Power Steering with H-infinity Control Designed to Obtain Road Information, In: *Proc. of the 1997 American Control Conference*, New Mexico, 1997.
- [17] A.T. Zaremba, M.K. Liubakka and R.M. Stuntz, Control and Steering Feel Issues in the Design of an Electric Power Steering System, In: *Proc. of the 1998 American Control Conference*, Pennsylvania, 1998.